Retinol-binding protein 2 (RBP2) binds monoacylglycerols and modulates gut endocrine signaling and body weight

Sueng-Ah Lee, Kryscilla Yang, Pierre-Jacques Brun, Josie Silvaroli, Jason Yuen, Igor Shmarakov, Hongfeng Jiang, Jun Feranil, Xueting Li, Atreju Lackey, et al.

MOLECULAR BIOLOGY

Retinol-binding protein 2 (RBP2) binds monoacylglycerols and modulates gut endocrine signaling and body weight

Seung-Ah Lee[1]*†, Kryscilla Jian Zhang Yang[1]*, Pierre-Jacques Brun[1]*, Josie A. Silvaroli[2], Jason J. Yuen[1], Igor Shmarakov[1], Hongfeng Jiang[1], Jun B. Feranil[1], Xueting Li[3], Atreju I. Lackey[4], Wojciech Krężel[5], Rudolph L. Leibel[6], Jenny Libien[7], Judith Storch[4], Marcin Golczak[2,8], William S. Blaner[1]*‡

Expressed in the small intestine, retinol-binding protein 2 (RBP2) facilitates dietary retinoid absorption. *Rbp2*-deficient (*Rbp2*$^{-/-}$) mice fed a chow diet exhibit by 6-7 months-of-age higher body weights, impaired glucose metabolism, and greater hepatic triglyceride levels compared to controls. These phenotypes are also observed when young *Rbp2*$^{-/-}$ mice are fed a high fat diet. Retinoids do not account for the phenotypes. Rather, RBP2 is a previously unidentified monoacylglycerol (MAG)-binding protein, interacting with the endocannabinoid 2-arachidonoylglycerol (2-AG) and other MAGs with affinities comparable to retinol. X-ray crystallographic studies show that MAGs bind in the retinol binding pocket. When challenged with an oil gavage, *Rbp2*$^{-/-}$ mice show elevated mucosal levels of 2-MAGs. This is accompanied by significantly elevated blood levels of the gut hormone GIP (glucose-dependent insulinotropic polypeptide). Thus, RBP2, in addition to facilitating dietary retinoid absorption, modulates MAG metabolism and likely signaling, playing a heretofore unknown role in systemic energy balance.

INTRODUCTION

Retinoids (vitamin A, its metabolites, and synthetic analogs) are potent transcriptional regulators of more than 500 diverse genes through the interaction of retinoic acid with its cognate nuclear hormone receptors (retinoic acid receptors, RARα, RARβ, and RARγ) (*1*, *2*). Abnormal signaling and deficits in both natural retinoids per se and a number of retinoid-binding proteins have been implicated in the development of metabolic disease (*3*), including obesity (*4*, *5*), insulin resistance (*6*), hepatic steatosis (*7*), and cardiovascular disease (*8*). Treatment of differentiating 3T3-L1 preadipocytes with all-*trans*-retinoic acid (ATRA) blocks further differentiation (*9*). Ablation of ATRA signaling through overexpression of a mutant dominant-negative RAR isoform results in hepatic steatosis when the transgene is expressed specifically in hepatocytes (*10*) and significantly diminishes glucose-stimulated insulin secretion when expressed specifically in pancreatic β cells (*11*). Loss of RARβ expression in hepatic stellate cells is associated with activation of these cells and the development of fibrotic disease (*12*, *13*). Retinol-binding protein 4 (RBP4), an adipokine that transports retinol in circulation, is proposed to link obesity with the development of impaired insulin responsiveness (*14*, *15*), excessive hepatic fat accumulation (*16*), and arterial wall disease (*17*). Elevated RBP4 concentrations in adipose tissue have been shown to increase adipose inflammation in a manner that is independent of RBP4 binding to retinol (*18*).

RBP2, also known as cellular RBP2 (CRBP2), is a member of the fatty acid–binding protein (FABP) family of intracellular lipid–binding proteins (*19*–*21*). It is expressed solely in the absorptive epithelium of the adult small intestine, most abundantly in the jejunum, where it binds all-*trans*-retinol or retinaldehyde and accounts for 0.4 to 1.0% of total soluble protein (*21*, *22*). Chylomicron production and fat absorption have not been extensively studied in *Rbp2*$^{-/-}$ mice. Only absorption of low and high doses of retinol provided in an oral fat challenge was assessed for these mice (*23*, *24*). In earlier studies of *Rbp2*$^{-/-}$ mice, we established that RBP2 channels newly absorbed retinol toward retinyl ester formation and incorporation into nascent chylomicrons (*24*). *Rbp2* also is transiently expressed in the neonatal liver and lung (*22*, *23*). *Rbp2*$^{-/-}$ dams, when maintained on a retinoid-sufficient diet, are reproductively normal (*23*).

We now report that RBP2 has a previously unsuspected role in the maintenance of body weight, normal responses to a glucose challenge, and normal fasting hepatic triglyceride (TG) levels. We show that human RBP2 binds monoacylglycerols (MAGs), including 2-arachidonoylglycerol (2-AG), 2-oleoylglycerol (2-OG), 2-lineoylglycerol (2-LG), and 1-AG with high affinity, comparable to that of retinol binding. The absence of *Rbp2* expression in mice alters 2-MAG concentrations in the proximal small intestine following an oral fat challenge. This is accompanied by significantly elevated blood levels of glucose-dependent insulinotropic polypeptide (GIP). We propose that the binding of the endocannabinoid 2-AG and/or other endocannabinoid-like 2-MAGs to RBP2 contributes toward maintaining normal enteroendocrine signaling, preventing development of the metabolic phenotypes observed in *Rbp2*$^{-/-}$ mice.

[1]Department of Medicine, Institute of Human Nutrition, College of Physicians and Surgeons, Columbia University, New York, NY, USA. [2]Department of Pharmacology, Case Western Reserve University, Cleveland, OH, USA. [3]PhD Program in Nutritional and Metabolic Biology, Institute of Human Nutrition, College of Physicians and Surgeons, Columbia University, New York, NY, USA. [4]Department of Nutritional Sciences and Rutgers Center for Lipid Research, Rutgers University, New Brunswick, NJ, USA. [5]Institut de Génétique et de Biologie Moléculaire et Cellulaire, U1258, CNRS, UMR 7104, Unistra, Illkirch 67404, France. [6]Department of Pediatrics, Institute of Human Nutrition, College of Physicians and Surgeons, Columbia University, New York, NY, USA. [7]Department of Pathology, SUNY Downstate Medical Center, Brooklyn, NY, USA. [8]Cleveland Center for Membrane and Structural Biology, Case Western Reserve University, Cleveland, OH, USA.
*These authors contributed equally to this work.
†Present address: Department of Molecular Medicine and Biopharmaceutical Sciences, Graduate School of Convergence Science and Technology, Seoul National University, Seoul 03080, Republic of Korea.
‡Corresponding author. Email: wsb2@cumc.columbia.edu

RESULTS

Rbp2 absence predisposes to excessive adiposity

During earlier studies of *Rbp2*$^{-/-}$ mice (*24*), we noticed a trend for 3- to 4-month-old male *Rbp2*$^{-/-}$ mice to have greater body weights than matched wild-type (WT) mice when the mice were maintained on a conventional chow diet; this trend did not reach statistical significance. However, by 6 to 7 months of age, male *Rbp2*$^{-/-}$ mice fed a chow diet throughout life showed significantly higher body weights than age-matched WT mice (Fig. 1A). Magnetic resonance imaging established that the increase in body weight was associated with a significant increase in body fat (Fig. 1B). Both the subcutaneous and visceral (VISC) fat pads from *Rbp2*$^{-/-}$ mice were significantly heavier than matched WT controls (Fig. 1C). Brown adipose tissue mass showed no genotype-dependent difference (Fig. 1C). The mean surface area of VISC adipocytes was greater in *Rbp2*$^{-/-}$ compared to WT mice (Fig. 1, D to F). The mean adipocyte size in *Rbp2*$^{-/-}$ mice was more than 30% greater compared to age-, gender-, and diet-matched WT mice (Fig. 1F). Calorimetry studies carried out at room temperature establish that during the light cycle, but not the dark cycle, 6- to 7-month-old chow-fed *Rbp2*$^{-/-}$ mice consume significantly less O_2 (Fig. 1G) but have similar respiratory exchange ratios (Fig. 1H) as WT mice. *Rbp2*$^{-/-}$ mice generate significantly less heat during the light cycle compared to WT controls (Fig. 1I). Food intake, monitored over a 5-day period, was also significantly lower, both in the light and dark cycles, in *Rbp2*$^{-/-}$ compared to matched WT mice (Fig. 1J). When we calculate from these data, the calories taken in by the mice and the calories being consumed, it becomes clear that the *Rbp2*$^{-/-}$ are consuming more calories than they are using. Thus, the balance between the decreased energy expenditure observed is not fully offset by lessened food intake for these mice. This is consistent with our observations of greater body weight gain as the *Rbp2*$^{-/-}$ mice age.

In *Rbp2*$^{-/-}$ mice fed a chow diet ad libitum for 6 to 7 months, fasting blood glucose and insulin concentrations were not different from WT mice, but intraperitoneal glucose clearance was impaired in *Rbp2*$^{-/-}$ mice (Fig. 2, A to C). Hepatic *Pepck* mRNA levels were elevated in chow-fed *Rbp2*$^{-/-}$ compared to matched WT mice (Fig. 2D), consistent with increased hepatic gluconeogenesis.

Fasting hepatic TG levels were significantly elevated in 6- to 7-month-old chow-fed male *Rbp2*$^{-/-}$ mice (Fig. 2E). Fasting plasma nonesterified fatty acid (FFA) concentrations were not different between chow-fed *Rbp2*$^{-/-}$ and WT mice (Fig. 2F). However, fasting plasma TG concentrations were significantly lower in *Rbp2*$^{-/-}$ mice (Fig. 2G). The diminished fasting plasma TG levels and elevated hepatic TG levels were associated with diminished rates of hepatic very-low-density lipoprotein (VLDL) secretion (Fig. 2H). Hepatic mRNA expression of *Fabp1* was elevated 1.3-fold; whereas expression of *Fabp2* and *Fabp4*, which are found at very low levels in liver relative to *Fabp1*, was unchanged (Fig. 2I). There were no detectable changes in mRNA expression of genes involved in hepatic lipogenesis including *Chrebp*, *Pparg*, *Fas*, *Scd1*, *Dgat1*, and *Dgat2*.

To better understand the metabolic phenotype of *Rbp2*$^{-/-}$ mice, groups of 2-month-old male *Rbp2*$^{-/-}$ and WT mice were fed either a high-fat diet providing 60% of calories from fat or a matched purified basal diet providing 10% of calories from fat. Both diets were formulated to have the same content of retinol. At the start of high-fat feeding, animals were tightly matched for age (53.0 ± 1.2 days for *Rbp2*$^{-/-}$ and 55.0 ± 1.1 days for WT mice) and body weight (24.8 ± 1.2 g for *Rbp2*$^{-/-}$ and 24.7 ± 1.3 g for WT mice). Both *Rbp2*$^{-/-}$ and WT mice fed the high-fat diet gained significantly more body weight than mice fed the basal diet (Fig. 3A). However, the *Rbp2*$^{-/-}$ mice fed the high-fat diet gained significantly more body weight than the WT mice fed that diet (Fig. 3A). This difference was statistically significant after 6 weeks of high-fat diet feeding, as the mice reached about 3 months of age. Dual-energy x-ray absorptiometry analysis confirmed that these differences were due primarily to significant increases in fat mass (Fig. 3B). After 8 weeks of feeding of the high-fat diet, impairments in glucose tolerance were apparent upon administration of an intraperitoneal glucose challenge (Fig. 3, C and D). However, no diet- or genotype-dependent differences in insulin sensitivity were observed (Fig. 3E).

We did not observe these adipose tissue or related phenotypes in female *Rbp2*$^{-/-}$ mice compared to gender-matched WT mice. Female *Rbp2*$^{-/-}$ mice are more resistant to the development of metabolic phenotypes than males, either when fed a chow diet for 6 to 7 months or a high-fat diet. Consequently, the remainder of the in vivo studies aimed at understanding these phenotypes used only male *Rbp2*$^{-/-}$ mice.

Metabolic dysregulation is not related to retinoid actions

Since the only proposed function for RBP2 is to facilitate intestinal uptake and intracellular transport of dietary and provitamin A carotenoid–derived retinol and retinaldehyde (*21*–*24*), we explored the effects of high-fat feeding on tissue retinoid homeostasis in these mice. Significantly higher hepatic concentrations of ATRA were observed in both *Rbp2*$^{-/-}$ and WT mice fed the high-fat diet, but no genotype-dependent differences were detected (fig. S1A). 9-*cis*-Retinoic acid was not detected in any liver sample. Hepatic expression of *Rarb*, a retinoic acid–responsive gene (*12*, *13*, *25*), was significantly elevated in high-fat diet–fed *Rbp2*$^{-/-}$ mice (fig. S1B). No genotype-dependent differences in mRNA levels of *Rbp4* or *Cyp26a1*, another gene whose expression is responsive to retinoic acid, were observed. Fasting plasma ATRA levels were significantly lower in *Rbp2*$^{-/-}$ fed the basal diet compared to WT mice but not different between *Rbp2*$^{-/-}$ and WT mice fed the high-fat diet (fig. S1C). Plasma RBP4 levels were elevated in high-fat diet–fed *Rbp2*$^{-/-}$ mice, probably reflecting the increased adiposity of these mice (fig. S1D). This finding was different from that for 7-month-old chow-fed *Rbp2*$^{-/-}$ mice whose circulating levels of RBP4 (fig. S1E) were not different from WT mice. Abdominal white adipose tissue total retinol (combined retinol and retinyl ester) levels were not statistically different between *Rbp2*$^{-/-}$ and WT mice fed either the high-fat or basal diet (fig. S1F). Unesterified retinol accounted for approximately 30 to 40% of the total retinol present in adipose tissue for each of the four groups. White adipose tissue mRNA expression levels for *Rbp4*, *Adipoq*, *Lep*, *Pgc1*, *Glut4*, *Ppara*, *Pparb*, and *Pparg* showed no genotype-dependent differences. For 7-month-old *Rbp2*$^{-/-}$ and WT mice fed the chow diet, 2 hours after administration of an oral bolus of a physiologic dose of retinol (6 μg) dissolved in 100 μl of corn oil, we observed no significant differences in plasma levels of ATRA (fig. S1G). Nor was 9-*cis*-retinoic acid detected in any of the postprandial sera. We observed no significant differences in levels of ATRA present in the proximal small intestines of *Rbp2*$^{-/-}$ and matched WT mice, either following a 5-hour fast or 2 hours after an oral gavage of 100 μl of corn oil that was preceded by a 5-hour fast (fig. S1H).

RBP2 binds 2-MAGs with high affinity

Since other members of the FABP protein family—those that bind FFA but not retinol—also bind 2-MAGs and the related *N*-acylethanolamines

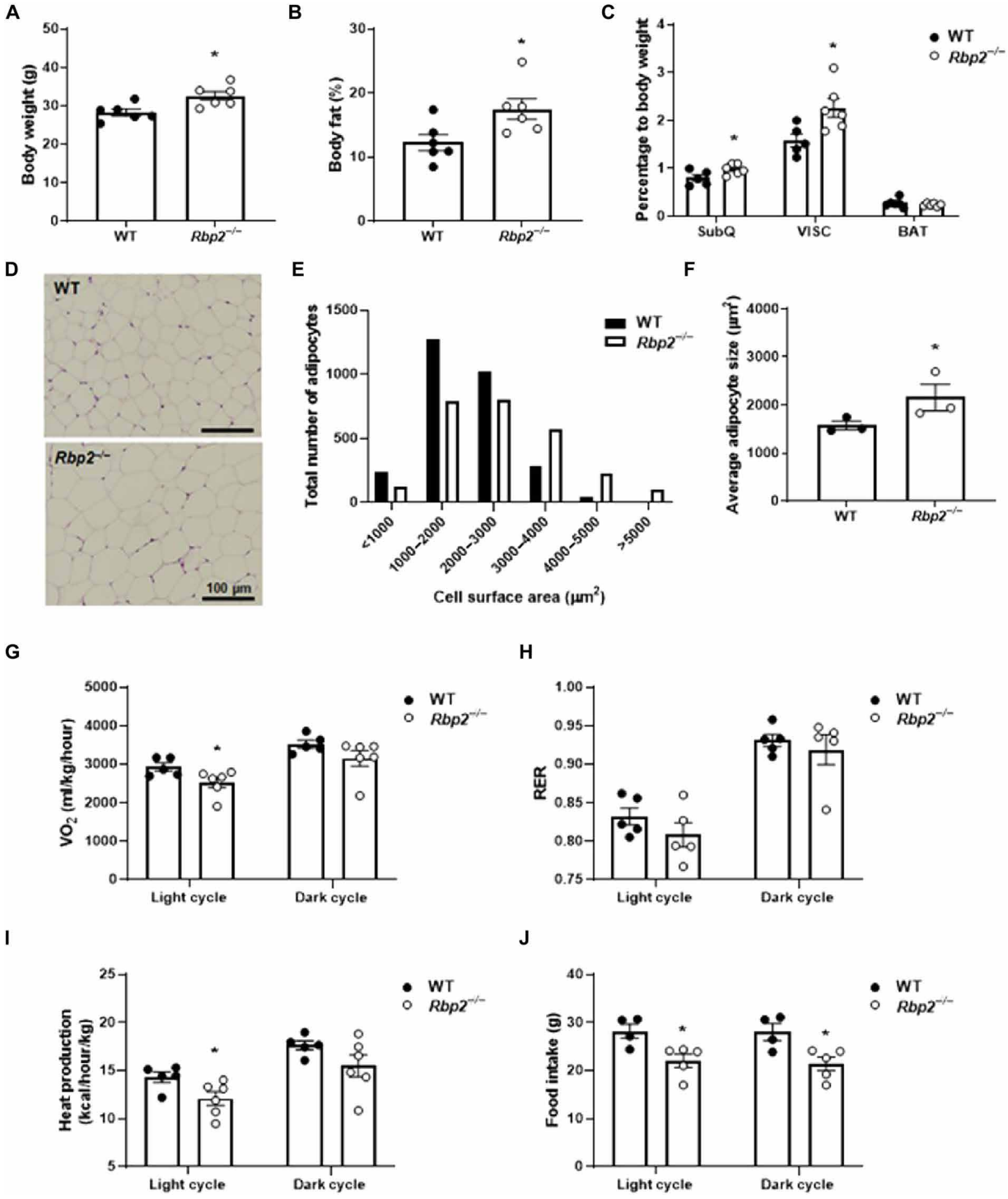

Fig. 1. *Rbp2*$^{-/-}$ mice gain more body fat than littermate controls as they age. (**A**) Six- to 7-month-old male *Rbp2*$^{-/-}$ mice fed a chow diet throughout life have a significantly greater body weight than matched controls fed the same diet. (**B**) Magnetic resonance imaging analysis shows that the increase in body weight is associated with significantly increased body fat. (**C**) A significant increase in fat mass was observed in both subcutaneous (SubQ) and VISC adipose tissue but not in brown adipose tissue (BAT). (**D**) Hematoxylin and eosin (H&E) staining of VISC (epididymal) adipose tissue establishes that adipocyte size in VISC fat was significantly larger for *Rbp2*$^{-/-}$ compared to control mice. (**E** and **F**) Adipocyte size distribution (E) and mean adipocyte size (F) for VISC adipose tissue from *Rbp2*$^{-/-}$ and matched WT mice. Adipocyte size was determined using multiple H&E-stained sections obtained from three *Rbp2*$^{-/-}$ and three matched WT mice. Calorimetry studies at room temperature undertaken on 6- to 7-month-old *Rbp2*$^{-/-}$ mice fed a chow diet throughout life establish that the *Rbp2*$^{-/-}$ mice consume significantly less O_2 during the light but not dark cycle (**G**) and have a similar respiratory exchange ratio (RER) to WT mice (**H**). *Rbp2*$^{-/-}$ mice generate significantly less heat during the light cycle compared to matched WT controls (**I**). Food intake monitored over a 5-day period is significantly lower, both in the light and dark cycles, in *Rbp2*$^{-/-}$ compared to matched WT mice (**J**). All data are presented as means ± SEM. Statistical significance: *$P < 0.05$.

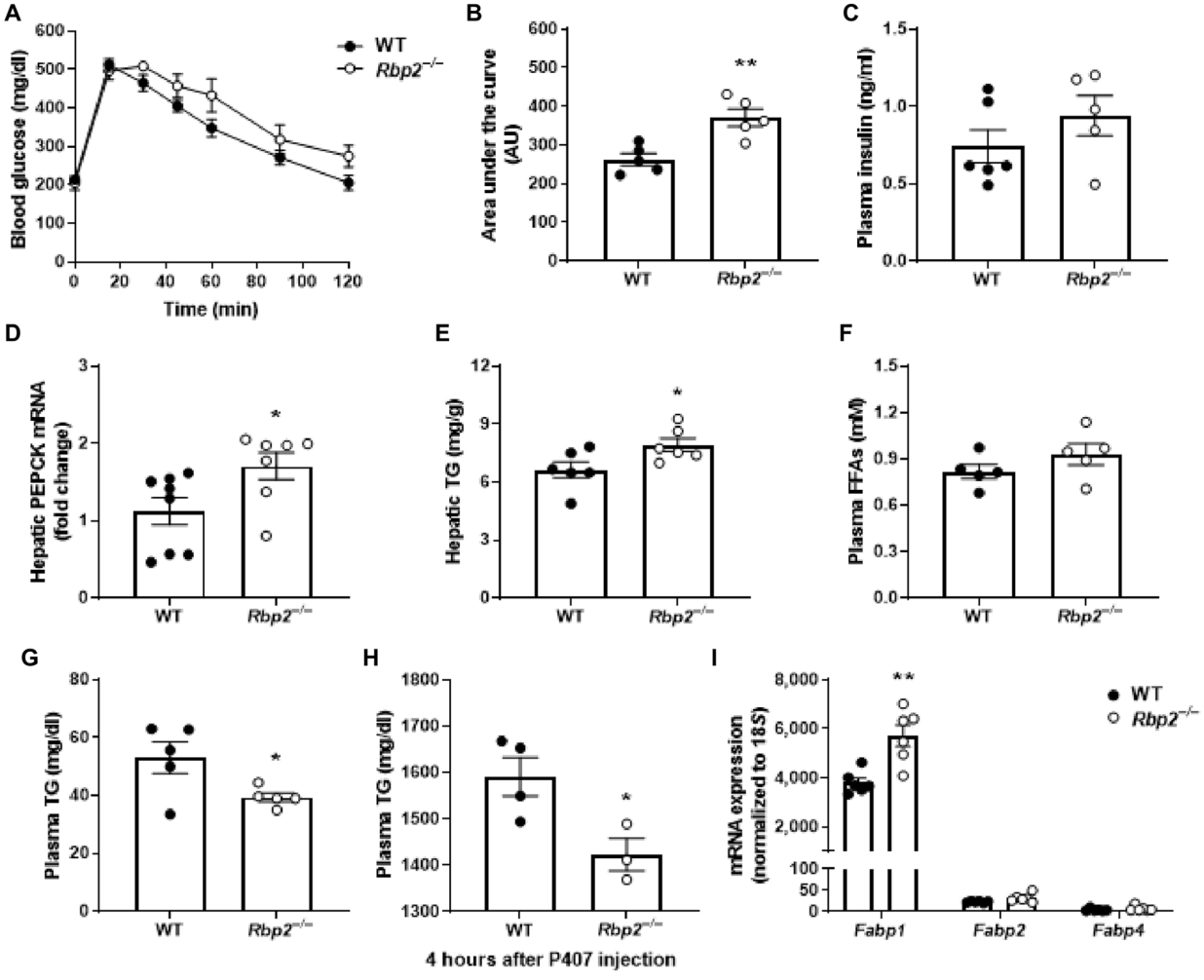

Fig. 2. Six- to seven-month-old *Rbp2*$^{-/-}$ mice maintained on a chow diet throughout life clear an intraperitoneal glucose challenge significantly less well than matched WT mice and have elevated fasting hepatic TG levels but lower plasma TG levels compared to matched WT mice. (**A**) Time course showing blood glucose levels in response to an intraperitoneal challenge of glucose for matched 6- to 7-month-old male *Rbp2*$^{-/-}$ and WT mice fed a chow diet throughout life. (**B**) The area under the glucose clearance curves (AUCs) for *Rbp2*$^{-/-}$ mice is significantly greater than that of matched WT mice. AU, arbitrary units. (**C**) Fasting plasma insulin levels are not different for matched *Rbp2*$^{-/-}$ and WT mice. (**D**) *Pepck* mRNA levels were elevated in fasting liver of *Rbp2*$^{-/-}$ mice compared to WT controls. (**E**) Fasting hepatic TG levels are significantly elevated in male *Rbp2*$^{-/-}$ mice. (**F** and **G**) Fasting plasma nonesterified fatty acid (FFA) levels are not different for matched *Rbp2*$^{-/-}$ and WT mice (F) but fasting plasma TG levels are significantly lower in the *Rbp2*$^{-/-}$ mice (G). (**H**) Livers of *Rbp2*$^{-/-}$ mice secrete significantly less TG bound to very-low-density lipoprotein (VLDL) than matched WT mice when P407 was used to block lipase action on newly secreted TG in VLDL. (**I**) Expression of *Fabp1* mRNA is elevated in livers of *Rbp2*$^{-/-}$ mice but no differences in expression levels of *Fabp2* or *Fabp4* were observed. All data are presented as means ± SEM. Statistical significance: **P* < 0.05 and ***P* < 0.01.

(NAEs) (*20*, *26*–*31*), we wondered whether RBP2 also might have some role in the metabolism of these bioactive lipids. To assess this possibility, we first undertook molecular modeling to determine whether 2-AG and *N*-arachidinoylethanolamine (AEA) are predicted to fit into the retinol-binding site of RBP2. 2-AG and AEA fit readily into the retinoid-binding pocket of RBP2. To assess directly the possibility that endocannabinoids and/or endocannabinoid-like substances bind RBP2, recombinant mouse RBP2 was purified. Incubation of holo-RBP2 with 2-AG, 2-OG, 1-AG, or 2-LG displaced retinol from its RBP2 binding pocket (Fig. 4A). By contrast, NAEs, including *N*-linoleoylethanolamine (LEA), *N*-myristoylethanolamine (MEA) and AEA, showed little displacement of RBP2-bound retinol (Fig. 4A). When recombinant apo-RBP2 was incubated with 2-AG, and the protein subsequently chromatographically repurified to remove unbound ligand, tandem mass spectrometry (MS/MS)–based detection established that 2-AG remained bound to RBP2 (Fig. 4B). The fluorescence emission spectra for retinol and the protein confirmed the finding that 2-AG, 2-OG, 1-AG, and 2-LG displace retinol and bind tightly to RBP2 (fig. S2, A to E). AEA was ~25-fold less effective than MAGs in displacing bound retinol from RBP2. The changes in fluorescence signal upon titration with the listed MAGs and NAEs were best fit with a one-site saturation binding model. The apparent binding constant (K_d) for 2-AG binding to RBP2, based on changes in protein fluorescence, was 27.1 ± 2.4 nM. For 2-OG, the apparent binding constant was 65.4 ± 4.4 nM. RBP2 was also found to bind tightly 2-LG (K_d = 40.0 ± 4.9 nM) and 1-AG (K_d = 21.0 ± 2.7 nM). AEA bound to RBP2 with a much lower affinity of K_d = 663.0 ± 24.0 nM (fig. S2F).

To obtain insight into the molecular aspect of these interactions, human RBP2 was cocrystallized with 2-AG [PDB (Protein Data Bank)

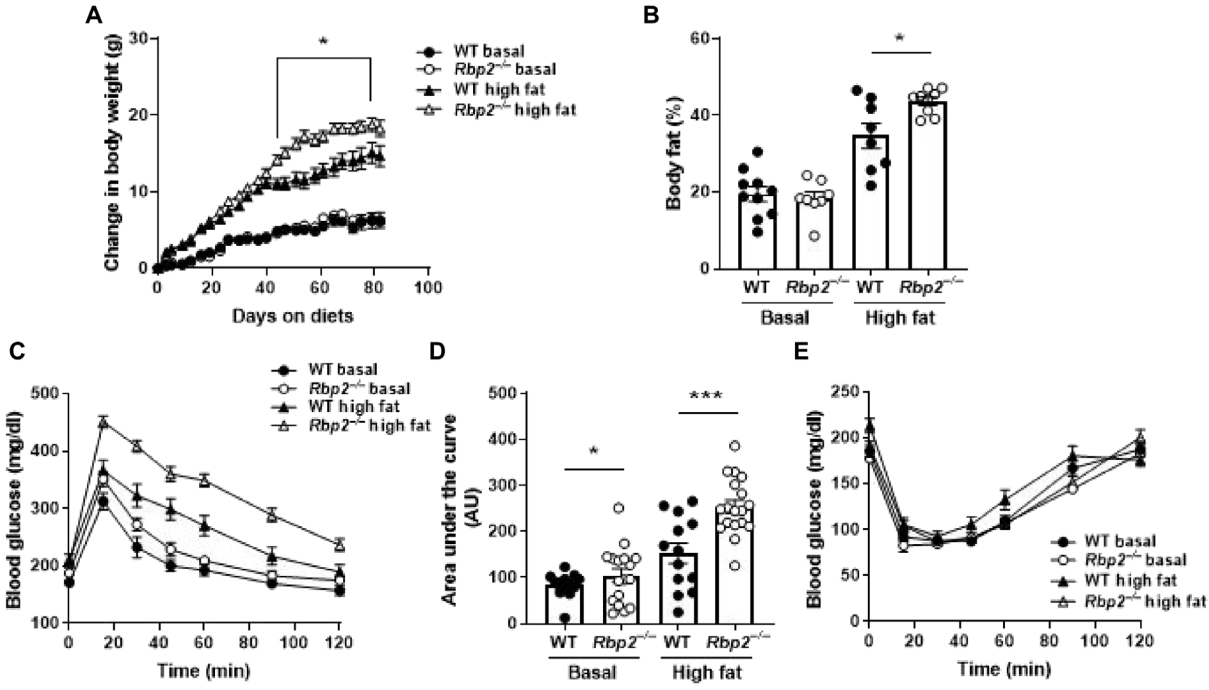

Fig. 3. When 7-week-old *Rbp2*$^{-/-}$ and matched WT mice are placed on a high-fat diet (60% of calories from fat), the *Rbp2*$^{-/-}$ mice gain significantly more body weight than WT. (**A**) Weight gain curves for *Rbp2*$^{-/-}$ and WT mice maintained on either a high-fat diet or a purified control diet (10% of calories from fat). (**B**) Upon 10 weeks of high-fat diet feeding, as determined by dual-energy x-ray absorptiometry, *Rbp2*$^{-/-}$ mice accumulate significantly more body fat than WT mice. (**C** and **D**) As seen from the plasma glucose clearance curves following an intraperitoneal challenge with glucose (C) and the resulting AUCs (D), the high-fat diet–fed *Rbp2*$^{-/-}$ mice respond significantly less well to the glucose challenge than WT mice. (**E**) The responses of matched *Rbp2*$^{-/-}$ and WT mice were not different following an intraperitoneal challenge with insulin. All data are presented as means ± SEM. Statistical significance: **P* < 0.05 and ****P* < 0.001.

6BTH] or AEA (PDB 6BTI), and the structures were solved at 1.35 and 1.45 Å, respectively (table S1). The electron densities for 2-AG or AEA were very well defined, allowing for unambiguous modeling of the lipid molecules inside the binding pocket of the protein (Fig. 4, C and D, and fig. S3, A and B). The endocannabinoids bind to the same site as retinol, and their spatial orientations resemble those observed for the retinoid moiety (Fig. 4, E and F). The polar end of the ligands is inserted deeply in the binding cavity, where it interacts with side chains of polar amino acids (Fig. 4C). Both the hydroxyl groups of 2-AG are involved in hydrogen bonding interactions (Fig. 4F). One of them is located in the proximity to K40 and Q108 forming hydrogen bonds with the ζ-nitrogen and ε-oxygen atoms of these side chains, whereas the other hydroxyl group interacts with the γ-hydroxyl of T51. The spatial orientation of the K40 side chain, critical for the interactions with 2-AG, is stabilized by a network of hydrogen bonds between the hydroxyl group of T53 and the water molecule (W3). In addition, the carbonyl oxygen of this endocannabinoid is part of an extended hydrogen bond network that involves water molecule W1 and side chains of Q97, E72, and Y60. Although all-*trans*-retinol and 2-AG interact with RBP2 with comparable affinities, their binding is achieved in different fashions dictated by the chemical composition of these ligands. With a single hydrogen bond donor, the interaction of all-*trans*-retinol depends predominantly on hydrophobic interactions that orient the β-ionone ring and the polyene chain within the binding pocket (Fig. 4F and fig. S3C). In contrast, the binding of 2-AG and related lipids relies on a network of hydrogen bonds that form between hydroxyl and carbonyl oxygen atoms and the side chains and ordered water molecules present in the cavity. Hydrophobic interactions do not contribute to the positioning of the acyl chain. Its orientation is largely defined by van der Waals forces. Because AEA contains only one hydroxyl group, the electron density for this ligand indicates two possible orientations for the hydroxyl end (fig. S3, A to C). They involve the interaction with either K40 and Q108 or T51, lowering the overall binding affinity of AEA as compared to 2-AG. The occupancy refinement indicated that projection of the hydroxyl toward the side chains of K40 and Q108 is more preferable.

Rbp2 affects GIP release by the intestine

Tight interactions of 2-AG, 2-OG, 1-AG, and 2-LG with RBP2 raise the possibility that RBP2 deficiency may influence MAG metabolism and actions. To explore this possibility, the concentrations of these MAGs were measured by liquid chromatography (LC)–MS/MS in the proximal small intestine (where RBP2 is most highly expressed) in mucosal scrapings obtained from age-matched *Rbp2*$^{-/-}$ and WT that had been maintained throughout life on a chow diet. The measures were carried out using tissue from older chow-fed mice initially fasted for 12 hours and then 2 hours following administration of an oral challenge with 100 μl of corn oil, a fat that is rich in both oleic and linoleic acids. Levels of 2-AG were significantly higher, by approximately 50%, in mucosal scrapings from *Rbp2*$^{-/-}$ mice (Fig. 5A). Similarly, mucosal levels of 2-LG and 2-palmitoylglycerol (2-PG) were also significantly elevated in mucosa from *Rbp2*$^{-/-}$ mice (Fig. 5, A and B). No statistically significant differences in 2-OG levels were observed (Fig. 5B). Nor did we detect differences in AEA levels between *Rbp2*$^{-/-}$ and WT intestines. Thus, RBP2, which localizes anatomically primarily to the jejunum, influences 2-MAG levels in the proximal small intestine following a fat challenge. For the same mice

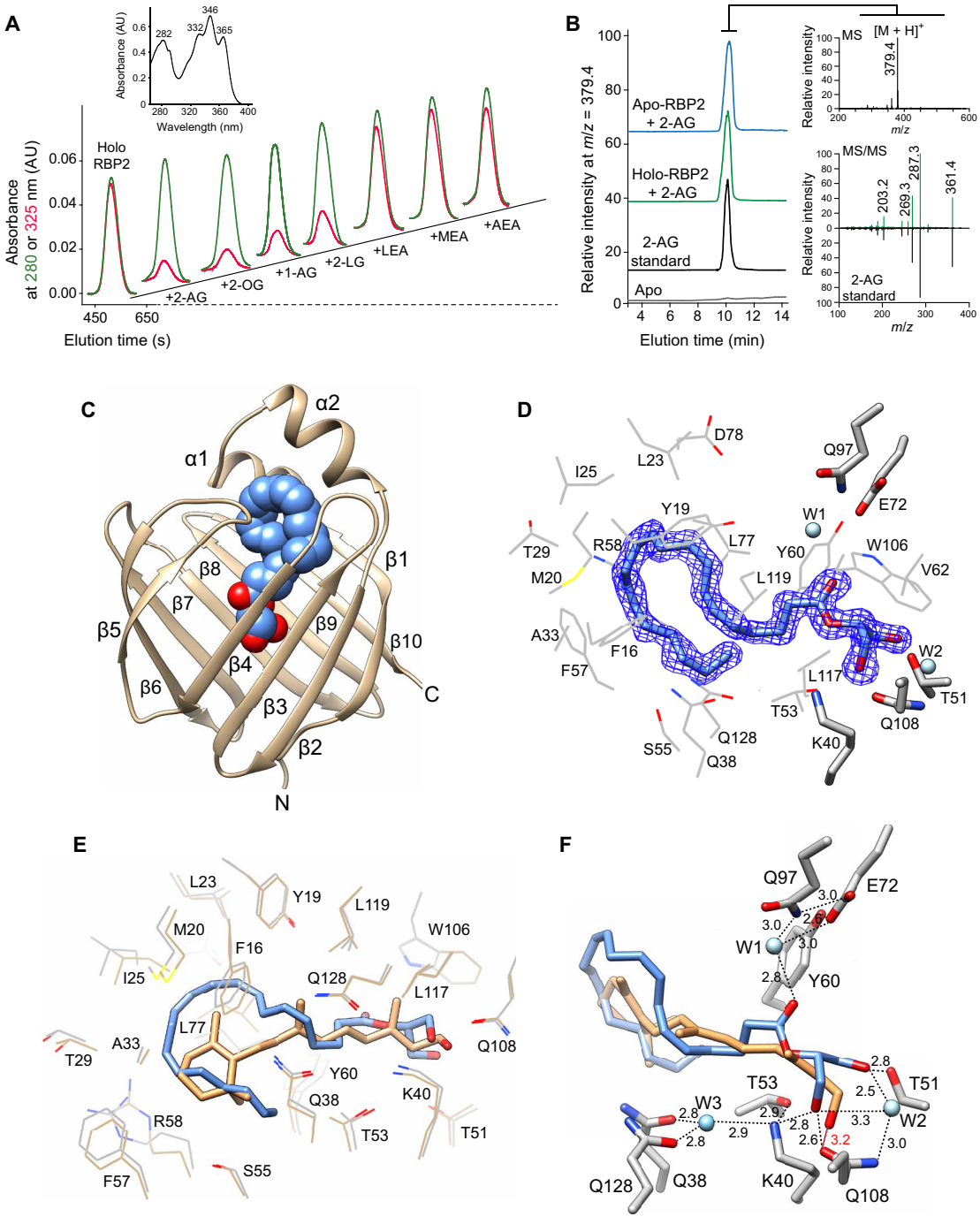

Fig. 4. RBP2 binds tightly 2-AG and 2-OG but not NAEs. (**A**) Incubation of holo-RBP2 with 2-AG, 2-OG, 1-AG, or 2-LG but not *N*-acylethanolamides (LEA, MEA, or AEA) leads to displacement of retinol from the binding site of RBP2. After incubation with tested ligands, the protein samples were repurified on an ion exchange column. The chromatograms represent elution profiles of RBP2 monitored at 280 nm (protein scaffold, green trace) and 325 nm (retinoid moiety, red trace). The inset shows the ultraviolet-visible absorbance spectrum for holo-RBP2. (**B**) Analysis of ethanolic extracts reveals the presence of an intense ion peak at mass/charge ratio (m/z) = 379.4 $[M + H]^+$ in the protein samples preincubated with 2-AG. The molecular identification of the m/z = 379.4 parent ion as 2-AG was achieved by comparing the MS/MS fragmentation pattern with a synthetic standard. (**C**) Ribbon diagrams of the RBP2 structure in complex with 2-AG. The position of the ligand within the binding pocket is indicated by a van der Waals surface model. (**D**) Molecular organization of the 2-AG–binding site with selected residues involved in formation of the internal cavity. Blue mesh signifies a refined $2F_o - F_c$ electron density map for the ligand at 1.4 σ. Carbon atoms of the ligand are colored blue, whereas oxygens are shown in red. Water molecules (W) are depicted as light blue spheres. (**E**) Comparison of the spatial orientation of the side chains and position of all-*trans*-retinol and 2-AG within the binding pocket. The overlay of structures of RBP2 in complex with all-*trans*-retinol (PDB 4QZT) and 2-AG (PDB 6BTH) indicates that the 2-AG occupies the same binding cavity as the retinoid by adopting a ring-like configuration of the acyl chain. (**F**) Details of the hydrogen bond network between 2-AG (shown in blue) or all-*trans*-retinol (shown in orange) and the polar side chain inside the ligand binding pocket. Both of the hydroxyl groups and the carbonyl oxygen of 2-AG are involved in numerous interactions with polar side chains, whereas hydrogen bonding of all-*trans*-retinol is limited to single interaction with the side chain of Q108. Distances between interacting atoms are in angstrom (Å).

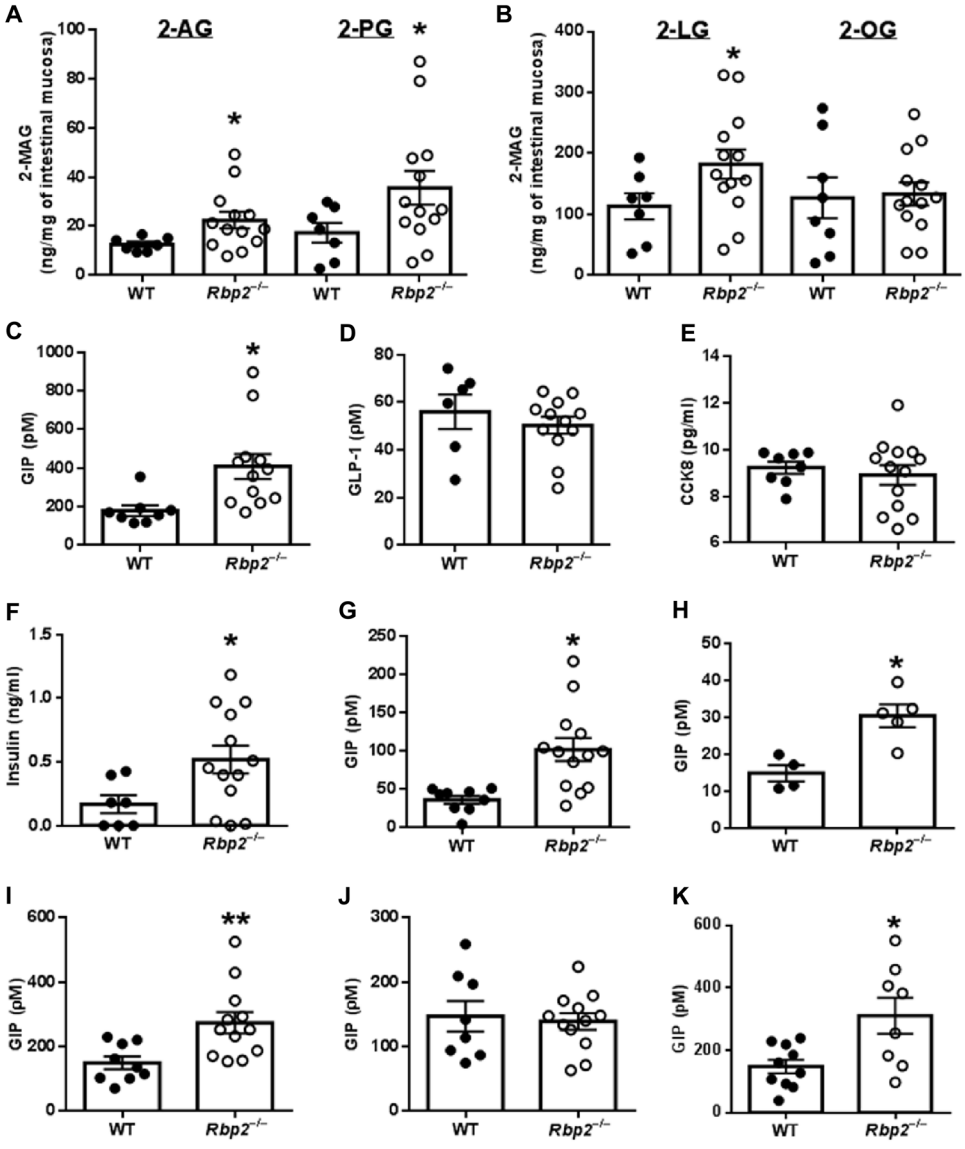

Fig. 5. Levels of 2-AG, 2-PG, 2-LG, and 2-OG in intestinal scrapings from the jejunum and plasma levels of GIP, GLP-1, CCK8, and insulin for *Rbp2*$^{-/-}$ and WT mice 2 hours after oral administration of a challenge of 100 μl of corn oil. (**A** and **B**) Levels of 2-AG, 2-PG, and 2-LG but not 2-OG were significantly elevated in mucosal scrapings obtained from *Rbp2*$^{-/-}$ mice. (**C** to **F**) Plasma levels of GIP (C) and insulin (F) but not GLP-1 (D) or CCK8 (E) were significantly elevated for *Rbp2*$^{-/-}$ mice receiving the corn oil challenge. (**G** and **H**) GIP levels present in plasma of both fed (G) and overnight fasting (H) *Rbp2*$^{-/-}$ mice were significantly elevated compared to those of matched WT mice. GIP levels were also significantly elevated in younger *Rbp2*$^{-/-}$ mice fed a high-fat diet for 8 weeks compared to matched WT mice in response to an oral fat challenge (**I**) but not in response to an oral glucose challenge (**J**). (**K**) Blood GIP levels were significantly elevated in *Rbp2*$^{-/-}$ mice when young (80 to 83 days old) *Rbp2*$^{-/-}$ and matched WT mice, which had been fed a chow diet throughout life, were challenged with 100 μl of corn oil. All data are presented as means ± SEM. Statistical significance: **P* < 0.05 and ***P* < 0.01.

used for MAG measurements, we also measured levels of GIP (Fig. 5C), glucagon-like peptide-1 (GLP-1) (Fig. 5D), cholecystokinin 8 (CCK8) (Fig. 5E), and insulin (Fig. 5F) in plasma obtained 2 hours after the fat challenge. Plasma levels of GIP for the *Rbp2*$^{-/-}$ mice were elevated by approximately twofold compared to the matched WT mice ($P < 0.05$). This was accompanied by a threefold elevation in insulin concentrations ($P < 0.05$). Plasma levels of GLP-1 and CCK8 following the fat challenge were not different between matched *Rbp2*$^{-/-}$ and WT mice. GIP levels in blood obtained from the fasted and fed *Rbp2*$^{-/-}$ and WT mice 1 week before their use for mucosal MAG measurements were also significantly elevated for *Rbp2*$^{-/-}$ mice both in the fed (Fig. 5G) and fasted (Fig. 5H) states ($P < 0.05$). No significant differences in plasma concentrations of either GLP-1 or CCK8 levels, in either the fasted or fed state, were observed between *Rbp2*$^{-/-}$ and WT mice.

In separate studies involving 3- to 4-month-old *Rbp2*$^{-/-}$ and WT mice fed a high-fat diet for 8 weeks, we observed a similar elevated GIP response to an oral challenge with 100 μl of corn oil for the *Rbp2*$^{-/-}$ mice (Fig. 5I) to the one we observed for older chow-fed mice (Fig. 5C). Unexpectedly, when these same mice were challenged a week later with oral glucose, we observed no differences between the GIP responses of *Rbp2*$^{-/-}$ and WT mice (Fig. 5J). Thus, RBP2 affects GIP release in response to fat but not glucose intake. When

younger (80 to 83 days old) *Rbp2*$^{-/-}$ and matched WT mice maintained throughout life on a chow diet were challenged with 100 μl of corn oil, the *Rbp2*$^{-/-}$ mice displayed significantly elevated blood GIP levels compared to WT mice (Fig. 5K). Since these younger chow-fed mice do not show differences in body weights or signs of other metabolic phenotypes, we conclude that the dysregulation of GIP release arising in the absence of *Rbp2* occurs before and not as a result of the excessive weight gain phenotype or any other metabolic phenotype.

Since RBP2 binds tightly to 2-MAGs, we also investigated expression levels of genes encoding proteins that are involved in MAG metabolism and actions within the small intestine (Fig. 6, A and B). Both *Fabp1* and *Fabp2* mRNA in the proximal small intestine of *Rbp2*$^{-/-}$ mice were elevated by approximately 1.6-fold, but no difference in the relatively low expression of *Fabp4* was observed (Fig. 6A). Expression levels in the proximal small intestine were determined for the cannabinoid receptors *Cb1* and *Cb2*, enzymes involved in NAE synthesis [*N*-acylphosphatidyl ethanolamine phospholipase D (*Nape-pld*) and degradation (fatty acid amide hydrolase (*Faah*)] and 2-MAG synthesis [diacylglycerol lipase b (*Dgl-b*) and degradation monoglyceride lipase (*Mgl*)] and a number of cell surface and nuclear receptors that are known to bind FFAs, NAEs, or 2-MAGs: *Cd36*, *Gpr119*, *Trpv1*, and *Ppara*. As shown in Fig. 6B, mRNA expression of *Dgl-b* and *Faah* was significantly reduced for *Rbp2*$^{-/-}$ mice. No statistically significant differences were observed for the other transcripts.

In limited investigations, we also asked whether the hypothalamus, the area within the central nervous system responsible for regulating energy expenditure and body weight, might express *Rbp2* or other RBPs. As expected, we did not detect *Rbp2* mRNA expression in whole hypothalamus obtained from chow-fed WT mice (Fig. 6C). However, we did observe considerable expression of *Rbp1* and lesser expression of *Rbp4* in this tissue. We also asked whether the absence of *Rbp2* expression in the intestine affected expression of hypothalamic genes involved in controlling food intake and energy expenditure (Fig. 6D). Expression of *Pomc* was significantly reduced in chow-fed 6- to 7-month-old male *Rbp2*$^{-/-}$ mice. However, no genotype-dependent differences in either *Agrp* or *Pyy* expression were observed.

DISCUSSION

Our data establish that as chow-fed male *Rbp2*$^{-/-}$ mice age they acquire more body fat, show an impaired response to a glucose challenge, and manifest elevated hepatic TG levels compared to diet-, age-, gender-, and genetic background–matched WT mice. Two-month-old *Rbp2*$^{-/-}$ mice fed a high-fat diet for 6 to 8 weeks similarly gain more body weight, display impaired glucose tolerance, and show higher fasting hepatic TG levels than age-matched WT mice. Aside from mediating retinol/retinaldehyde trafficking within the intestinal mucosa (*21*–*24*), as far as we are aware, RBP2 has not previously been implicated as having other physiological actions. With this understanding of RBP2 actions in the body, it is thus unexpected that a null mutation in *Rbp2* would give rise to the increased adiposity and the other metabolic phenotypes we have observed. When Ong (*19*) first identified RBP2 more than three decades ago, he showed that exogenous retinol added to a tissue homogenate copurified with RBP2 protein to homogeneity. This was taken to indicate that retinol or its oxidized form, retinaldehyde, is the endogenous ligands for RBP2. For the adult intestine, it has been estimated that RBP2 represents 0.4 to 1.0% of total soluble protein (*21*, *22*). This raises a puzzling question as to why such a large quantity of this protein would be needed solely to facilitate retinol/retinaldehyde uptake, which in mice normally amounts to less than 10 μg/day (*32*). We now report that RBP2 binds MAGs

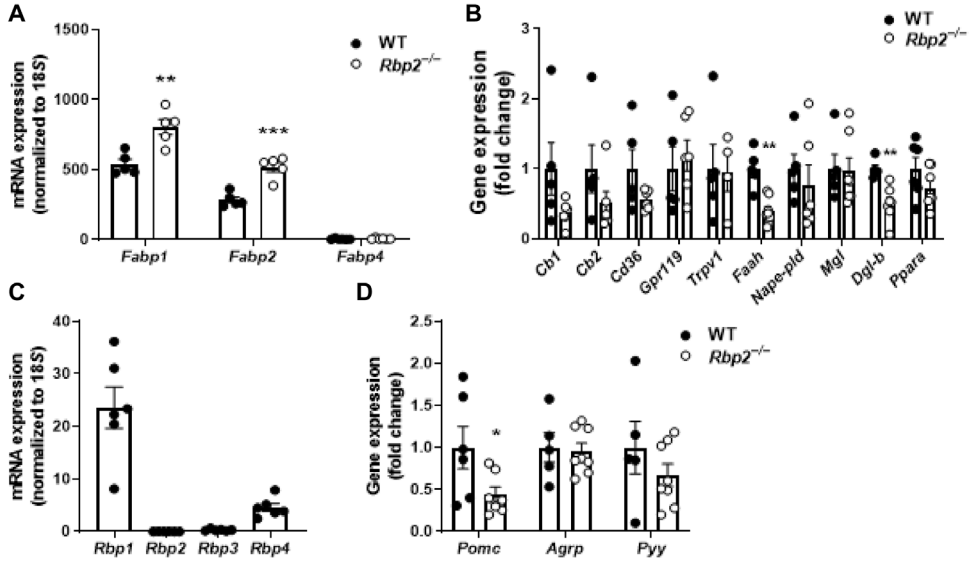

Fig. 6. The absence of Rbp2 alters expression of genes in the intestine and hypothalamus. (**A**) Expression of both *Fabp1* and *Fabp2* but not *Fabp4* are significantly elevated in the proximal portion of the small intestine for *Rbp2*$^{-/-}$ mice compared to WT. (**B**) Expression levels in the proximal small intestine were assessed for the endocannabinoid receptors *Cb1* and *Cb2*, enzymes involved in NAE synthesis [*N*-acylphosphatidyl ethanolamine phospholipase D (*Nape-pld*) and degradation (fatty acid amide hydrolase (*Faah*)] and 2-MAG synthesis [diacylglycerol lipase b (*Dgl-b*) and degradation (monoglyceride lipase (*Mgl*)] and a number of cell surface and nuclear receptors that are known to bind FFA, NAEs, or 2-MAGs (*Cd36*, *Gpr119*, *Trpv1*, and *Ppara*). mRNA expression of *Dgl-b* and *Faah* was significantly reduced for *Rbp2*$^{-/-}$ mice, but no statistically significant differences were observed for the other transcripts. (**C**) RBP2 is not expressed in the hypothalamus of WT mice fed a chow diet. However, both *Rbp1* and *Rbp4* are expressed in the hypothalamus. (**D**) The absence of *Rbp2* expression in the small intestine is associated with significantly diminished expression of the *Pomc* gene in the hypothalamus but has no effect on either *Agrp* or *Pyy* gene expression. All data are presented as means ± SEM. Statistical significance: **P* < 0.05, ***P* < 0.01, and ****P* < 0.001.

and endocannabinoids, 2-AG, 2-OG, 2-LG, and 1-AG with high affinity, with the same order of magnitude as that of retinol binding and that the absence of RBP2 in the intestine increases enterocyte 2-MAG concentrations following a fat challenge. Consequently, RBP2 acts physiologically within the intestinal mucosa as a MAG-binding protein. Intestinal MAG concentrations following a conventional meal will be several orders of magnitude greater than that of retinol. This previously unrecognized function likely accounts for the high expression level of RBP2 in the intestine.

What accounts for the age- and diet-dependent increase in body fat, glucose insensitivity, and elevated fasting hepatic TG levels observed for male *Rbp2*$^{-/-}$ mice? Given the central role of RBP2 in the intestinal uptake and processing of dietary retinol/retinaldehyde (*21*–*24*), we initially considered whether *Rbp2* deficiency may affect retinoid homeostasis throughout the body. *Rbp2*$^{-/-}$ mice are not retinoid deficient when maintained on a chow diet (*23*). These mice maintain normal serum retinol levels despite hepatic stores of total retinol (unesterified retinol and retinyl ester) being reduced by 40% in *Rbp2*$^{-/-}$ mice (*23*). Possibly though, there may be some unsuspected role for RBP2 in the maintenance of retinoic acid levels within the body, and tissue levels of retinoic acid had not been previously studied in *Rbp2*$^{-/-}$ mice. We did not detect genotype-dependent differences in ATRA levels in liver, in white adipose tissue, or in fasting and nonfasting intestinal tissue or plasma. In agreement with the literature (*33*), we did not detect 9-*cis*-retinoic acid in any of these tissues. We did observe an effect of feeding a high-fat diet on lowering ATRA levels in brown adipose tissue, but this effect was observed in both *Rbp2*$^{-/-}$ and WT mice. Modest but significant increases in hepatic mRNA levels of the retinoic acid–responsive *Rarb* and *Pepck* genes (*12*, *25*) were detected (Fig. 2D and fig. S1B), but no other differences were observed for genes associated with hepatic retinoid metabolism or actions. No genotype-dependent differences in expression levels of retinoid-related genes were observed in either white or brown adipose tissue. Collectively, these data argue against the possibility that the absence of RBP2 has effects on whole-body retinoid homeostasis or actions that account, per se, for the metabolic phenotypes observed in *Rbp2*$^{-/-}$ mice. However, our data do not definitively rule out the possibility that retinoids or some other factors may be involved in the development of the phenotypes we observed.

A more likely explanation for the metabolic phenotypes observed for *Rbp2*$^{-/-}$ mice involves a role for RBP2 in trafficking and metabolism of MAGs. This role could involve the actions of RBP2 in facilitating bulk lipid uptake from the diet or 2-MAG signaling. MAGs generated in the intestinal lumen from dietary TGs are taken up by enterocytes where they are used primarily to resynthesize TGs that are then incorporated into nascent chylomicrons (*34*, *35*). Some MAGs will be degraded by MAG lipase to nonesterified fatty acids that may be used for TG synthesis and incorporation into chylomicrons (*35*, *36*). It is possible that RBP2 plays a role in metabolically trafficking MAGs toward TG synthesis and chylomicron formation. This putative action of RBP2 could affect both the quantity of TG incorporated into chylomicrons and the acyl composition of chylomicron lipids.

In addition, 2-MAGs are potent signaling molecules acting as agonists for the cell surface receptor GPR119 that is present on the enteroendocrine K and L cells found in the small intestine (*37*–*39*). GPR119 is known to signal enteroendocrine cell release of GIP and GLP-1 in both rodents and humans, affecting metabolism and energy expenditure (*37*–*39*). 2-AG is a canonical endocannabinoid and is able to bind and activate cannabinoid receptors 1 and 2 (CB1 and CB2) (*40*). A recent study in humans concluded that elevated GIP levels in obesity are likely a consequence of increased gut endocannabinoid levels (*41*). Several other studies have reported elevated blood GIP levels in obese humans (*42*, *43*). Elevated GIP levels have been reported in diet-induced obese mice (*44*). Genetically modified mice lacking an intact cell surface receptor for GIP are protected from obesity associated with high-fat diet consumption, leptin deficiency, and ovariectomy (*43*–*47*). GIP is reported to exert direct effects on adipocytes including the enhancement of lipoprotein lipase transcription and activity facilitating fatty acid uptake from the postprandial circulation by adipocytes and the suppression of intracellular lipolysis (*48*, *49*). Our data indicate that plasma GIP levels, but not GLP-1 levels, are elevated in *Rbp2*$^{-/-}$ mice after administration of a challenge with 100 μl of corn oil (Fig. 5). Moreover, this elevated GIP response is seen in young chow-fed mice before there is any evidence of an excessive weight gain or other metabolic phenotype. We propose that the simplest explanation for the higher weight gain and impaired glucose clearance observed in *Rbp2*$^{-/-}$ mice is that this arises due to increased intestinal 2-MAG concentrations affecting enteroendocrine cell release of GIP and subsequent GIP-induced alterations in lipid and carbohydrate metabolism in the periphery, particularly in adipose tissue.

MAG-dependent signals originating from the gut are known to have systemic effects involving many tissues including the hypothalamus, which controls eating behavior and energy expenditure (*50*, *51*). We observed significantly reduced expression of *Pomc*, an anorexigenic neuropeptide (*52*), in hypothalamus obtained from chow fed 6- to 7-month-old male *Rbp2*$^{-/-}$ compared to matched WT mice. No genotype-dependent differences in either *Agrp* or *Pyy* expression were observed. Nevertheless, these data suggest differences between *Rbp2*$^{-/-}$ and WT mice in hypothalamic signaling pathways. Although, at the present time, we have not investigated in any depth this possibility, we anticipate that further study of how the absence of *Rbp2* expression in the intestine affects hypothalamic pathways—possibly via direct vagus-mediated traffic into the brain–will be needed to understand fully the actions of RBP2 in maintaining normal metabolic health.

The FABP protein family comprises nine known 14- to 15-kDa intracellular proteins that bind FFAs with high affinity (*20*, *53*, *54*). In addition, the FABP family also includes three intracellular RBPs (RBP1, RBP2, and RBP7) and two intracellular retinoic acid–binding proteins (CRABP1 and CRABP2) (*20*, *22*, *53*, *54*). Until the present study, none of the retinoid-binding proteins had been shown to bind with high-affinity ligands other than retinol, retinaldehyde, or retinoic acid. However, a number of FABPs are reported to bind strongly to 2-MAGs or NEAs (*20*, *27*, *28*, *30*), and this, in turn, influences the levels of these compounds in cells and tissues. Kaczocha *et al.* (*26*, *29*) demonstrated elevated rates of AEA uptake into cells overexpressing either FABP5 or FABP7 but not FABP3. These authors further proposed that FABPs mediate the intracellular delivery of endocannabinoids or NEAs either to inactivating enzymes or to the nucleus where they can activate peroxisome proliferator–activated receptor α (*26*). FABP1 binds strongly 2-MAGs, with an apparent dissociation constant for 2-OG binding of approximately 65 nM (*28*). It also has been reported that *Fabp1*$^{-/-}$ mice have significantly diminished hepatic levels of *N*-oleoylethanolamine (OEA), *N*-palmitoylethanolamine, and AEA and lower serum levels of OEA but unchanged mucosal OEA levels, suggesting a possible role for FABP1 in NAE metabolic processing (*27*). These published observations for other FABP protein

family members are similar to ours, in which we have observed strong binding of MAGs to RBP2, with K_d values in the 25 to 60 nM range, and elevated 2-MAG levels in the proximal small intestine of *Rbp2*$^{-/-}$ mice following oral administration of a corn oil challenge. We propose that RBP2 acts within the intestinal mucosa as a binding protein for 2-MAGs such as 2-AG, 2-LG, 2-OG, and 2-PG, or 1-AG, regulating their functional intracellular concentrations, likely by facilitating either degradation, modulating their incorporation into triacylglycerol or phospholipid and/or regulating their trafficking to receptors involved in signal transduction and energy homeostasis.

Many reports have established FABPs as important modulators of metabolism and inflammatory processes and, consequently, contributors to metabolic disease development and prevention (*53*, *54*). Mice deficient in *Fabp1*, when fed a high-fat diet rich in long-chain saturated fatty acids, display significantly greater body weights and fat masses compared to matched WT mice (*20*, *55*). When mice lacking *Fabp2* are fed this same diet, they remain lean, with lower body weights and fat masses than WT mice (*20*, *55*). Consistent with these experimental studies, polymorphisms in both the human *FABP1* and *FABP2* genes have been associated with increased incidence of obesity and glucose intolerance (*30*). FABP1, in addition to being highly expressed in the liver, is abundantly expressed in intestinal absorptive cells, as is FABP2. Both FABPI and FABP2 are expressed abundantly in jejunum, as is RBP2. Our finding that RBP2 is an intestinal MAG-binding protein is thus somewhat puzzling. Unlike FABP1, RBP2 does not bind FFAs. However, both RBP2 and FABP1 are MAG-binding proteins that colocalize to the same anatomical region of the small intestine (the jejunum). Are their functions in MAG trafficking redundant or does each protein have a unique metabolic action within the enterocyte? Moreover, *Rbp2*$^{-/-}$, *Fabp1*$^{-/-}$, and *Fabp2*$^{-/-}$ mice each display clear adiposity phenotypes when challenged with a high-fat diet. Do these phenotypes all arise due to effects of these proteins on the same pathway or through multiple different pathways? Since MAGs can displace retinol from its binding site in RBP2, this raises an important question regarding how RBP2 facilitates both retinol and MAG absorption and/or metabolism. Following a fat-rich meal, intestinal concentrations of 2-MAGs will normally be several orders of magnitude greater than those of retinol/retinaldehyde, yet the K_d values for retinol and retinaldehyde binding (*33*) are two to six times higher than those that we report here for 2-MAG binding. Does the quality and/or quantity of dietary fat influence retinol-RBP2 interactions in a manner that affects retinoid absorption mediated by RBP2? Or is the concentration of RBP2 within enterocytes sufficient to accommodate both retinoid and MAG absorption and metabolism? Understanding of these issues will be important for understanding RBP2 actions in intestinal neutral lipid metabolism and nutrient sensing.

In summary, we have identified a previously unidentified biochemical function for human RBP2 that involves binding of the endocannabinoid 2-AG and related endocannabinoid-like 2-MAGs that have been implicated in the maintenance of normal body weight and glucose homeostasis in mice. When RBP2 is absent, body weight and glucose homeostasis are adversely affected. At the level of the enterocyte, these phenotypes are associated with altered regulation of GIP synthesis and/or release from enteroendocrine cells into the circulation where it can affect adiposity. Our work raises a number of fundamental questions regarding how RBP2 may be acting in the biology of MAGs, both within the small intestine and systemically. However, a number of hurdles remain before these findings can be used to understand and treat human disease. We do not yet understand the molecular basis for altered enterocyte levels of 2-MAGs in response to an oral fat challenge and the associated elevations in GIP levels in blood. It is unclear whether this involves a direct mechanism that affects enteroendocrine cells through only local actions within the intestine. Or if these effects involve the gut-brain axis and central nervous system input into the regulatory process. These possibilities need to be resolved. In addition, we will need to gain understanding of the role of RBP2 in human intestinal physiology and enteroendocrine signaling, extending our work in the mouse. These key limitations are planned foci for future investigation of RBP2 actions in 2-MAG metabolism and intestinal enteroendocrine signaling.

MATERIALS AND METHODS

Study design

While undertaking earlier work investigating the role of RBP2 in metabolically channeling newly absorbed retinol to lecithin:retinol acyltransferase (LRAT) for esterification and incorporation into nascent chylomicrons (*24*), we noted that 4- to 5-month-old *Rbp2*$^{-/-}$ mice congenic in the C57BL/6J genetic background and maintained on a conventional chow diet tended to have greater body weights than age- and gender-matched WT mice. To better understand this, we placed 2-month-old male *Rbp2*$^{-/-}$ and matched littermate controls on a high-fat diet and observed their weights. The *Rbp2*$^{-/-}$ mice quickly gained significantly more body weight than WT mice (Fig. 3), suggesting a role for RBP2 in the regulation of the body weight. Moreover, weight gain was associated with the induction of glucose intolerance. Going back to our original observation, when *Rbp2*$^{-/-}$ were fed a chow diet for 6 to 7 months of age, we also observed a statistically significant elevation in the body weights of the mutant mice. Since the literature suggests a role for retinoids and/or retinoid-related proteins in preventing and/or contributing to metabolic disease, we initially focused on the possibility that retinoid actions might account for these observations. We obtained no direct evidence supporting this notion (fig. S1). Earlier, we had undertaken studies investigating the structural properties of LRAT and the five other related vertebrate members of this protein family (*56*). The other vertebrate members of this protein family act biochemically as either acyltransferases or phospholipases (*56*, *57*). A number of these LRAT-like proteins are reported to have catalytic roles leading to the formation of NAEs or other bioactive lipids (*56*, *57*). Hence, we wondered whether, analogous to RBP2's actions in metabolically channeling retinol to LRAT, RBP2 might bind other lipids and metabolically channel these to an LRAT-like protein(s) leading to an effect on the formation of other bioactive lipids that regulate body weight. This possibility was investigated by testing several classes of endogenous lipid molecules. Binding of lipid could be readily monitored by following the decline in retinol fluorescence as it is displaced from its binding pocket. Using this approach, we were successful in establishing that 2-MAGs bind RBP2 with high affinity (Fig. 4 and fig. S2). We then asked whether the absence of RBP2 affected 2-MAG levels in the intestine and intestinal biology. As we report, both are very significantly affected by the RBP2 absence.

All nutritional and biochemical studies were designed to assure that we were able to detect statistically significant differences of 20% or more with a level of confidence of 5% or greater. Since, initially, we were unsure as to what differences in body weight gains we might

expect in the high-fat diet feeding studies, we used relatively large groups of mice consisting of 16 to 18 mice per group. For the high-performance LC and LC/MS/MS measurements of retinoids or 2-MAGs, the needed group sizes were determined on the basis of our earlier published work (*58*, *59*). Standard commercial kits were used for the measurement of glucose, insulin, and gut hormones. All mice were bred, raised, fed a high-fat diet, or otherwise manipulated in the Columbia University Medical College Animal Facility. Ligand binding and crystallographic studies were carried out at Case Western Reserve University. Full Worldwide Protein Data Bank (wwPDB) X-ray Structure Validation Reports are available online for RBP2 binding to 2-AG (PDB 6BTH) and to AEA (PDB 6BTI). *Rbp2*$^{-/-}$ mice will be provided to investigators at their request. Similarly, upon request, we will make available all information regarding specific aspects of technical protocols used in our work or other requested information relating to the work.

Statistical analysis

All data are presented as means ± SEM. Data were analyzed for statistical significance using standard procedures consisting of an unpaired *t* test for comparisons of two groups or an analysis of variance (ANOVA), followed by post hoc analysis if more than two groups of mice were being compared. All data obtained from measures were included in statistical calculations. Statistically significant differences were noted for $P < 0.05$.

Animals, animal husbandry, and diets

The *Rbp2*$^{-/-}$ mice used in our studies were all males and congenic on the C57BL/6J genetic background. These mice were originally described by E *et al.* (*23*). For our studies, we used age- and diet-matched male littermates that were generated from crosses of heterozygotes progeny obtained from crosses of these original *Rbp2*$^{-/-}$ with C57BL/6J mice. The mice were maintained on a 12-hour dark-light cycle, with the period of darkness between 7:00 p.m. and 7:00 a.m. in a conventional barrier facility. Mice, regardless of diet treatment, were provided both diet and water ad libitum. All animal experiments were conducted in accordance with the National Research Council's Guide for the Care and Use of Laboratory Animals (*60*) and were approved by the Columbia University Institutional Animal Care and Use Committee.

For studies involving mice that had been maintained only on a conventional chow diet throughout life, we routinely studied mice that were 6 to 7 months of age. For high-fat diet feeding studies, mice were placed on a high-fat diet commencing at approximately 2 months of age and were maintained on the high-fat diet for up to 16 weeks. Before the start of high-fat feeding studies, mice were maintained throughout life on a conventional chow diet providing 15 IU vitamin A/g diet. The high-fat diet used in our studies was obtained from Research Diets (New Brunswick, NJ) (diet number D12492) and provided 60% of calories as fat and 5.2 IU vitamin A/g diet. The control mice were fed a basal purified diet (Research Diets, D12450B) providing 10% of calories from fat and 3.8 IU vitamin A/g diet. Body weights were measured two times a week throughout the high-fat feeding period.

SUPPLEMENTARY MATERIALS

Supplementary material for this article is available at http://advances.sciencemag.org/cgi/content/full/6/11/eaay8937/DC1

Supplementary Materials and Methods

Fig. S1. Lack of differences in ATRA levels in tissues and in circulating RBP4 levels between basal control and high-fat diet–fed *Rbp2*$^{-/-}$ and WT mice.

Fig. S2. Determination of K_d values for interaction of RBP2 with MAGs and AEA.

Fig. S3. Position of AEA inside the binding pocket of RBP2 and comparison of the modes of binding for all-*trans*-retinol, 2-AG, and AEA.

Table S1. X-ray data collection and refinement statistics.

References (*61*–*70*)

View/request a protocol for this paper from *Bio-protocol*.

REFERENCES AND NOTES

1. J. E. Balmer, R. Blomhoff, Gene expression regulation by retinoic acid. *J. Lipid Res.* **43**, 1773–1808 (2002).
2. Z. Al Tanoury, A. Piskunov, C. Rochette-Egly, Vitamin A and retinoid signaling: Genomic and nongenomic effects. *J. Lipid Res.* **54**, 1761–1775 (2013).
3. W. S. Blaner, Vitamin A signaling and homeostasis in obesity, diabetes, and metabolic disorders. *Pharmacol. Ther.* **197**, 153–178 (2019).
4. F. Preitner, N. Mody, T. E. Graham, O. D. Peroni, B. B. Kahn, Long-term fenretinide treatment prevents high-fat diet-induced obesity, insulin resistance, and hepatic steatosis. *Am. J. Physiol. Endocrinol. Metab.* **297**, E1420–E1429 (2009).
5. N. Noy, The one-two punch: Retinoic acid suppresses obesity both by promoting energy expenditure and by inhibiting adipogenesis. *Adipocyte* **2**, 184–187 (2013).
6. H. Tsuchiya, Y. Ikeda, Y. Ebata, C. Kojima, R. Katsuma, T. Tsuruyama, T. Sakabe, K. Shomori, N. Komeda, S. Oshiro, H. Okamoto, K. Takubo, S. Hama, K. Shudo, K. Kogure, G. Shiota, Retinoids ameliorate insulin resistance in a leptin-dependent manner in mice. *Hepatology* **56**, 1319–1330 (2012).
7. S. E. Trasino, X.-H. Tang, J. Jessurun, L. J. Gudas, Retinoic acid receptor β2 agonists restore glycaemic control in diabetes and reduce steatosis. *Diabetes Obes. Metab.* **18**, 142–151 (2016).
8. D. Bilbija, A. A. Elmabsout, J. Sagave, F. Haugen, N. Bastani, C. P. Dahl, L. Gullestad, A. Sirsjö, R. Blomhof, G. Valen, Expression of retinoic acid target genes in coronary artery disease. *Int. J. Mol. Med.* **33**, 677–686 (2014).
9. E. J. Schwarz, M. J. Reginato, D. Shao, S. L. Krakow, M. A. Lazar, Retinoic acid blocks adipogenesis by inhibiting C/EBPbeta-mediated transcription. *Mol. Cell. Biol.* **17**, 1552–1561 (1997).
10. A. Yanagitani, S. Yamada, S. Yasui, T. Shimomura, R. Murai, Y. Murawaki, K. Hashiguchi, T. Kanbe, T. Saeki, M. Ichiba, Y. Tanabe, Y. Yoshida, S. Morino, A. Kurimasa, N. Usuda, H. Yamazaki, T. Kunisada, H. Ito, Y. Murawaki, G. Shiota, Retinoic acid receptor α dominant negative form causes steatohepatitis and liver tumors in transgenic mice. *Hepatology* **40**, 366–375 (2004).
11. P.-J. Brun, A. Grijalva, R. Rausch, E. Watson, J. J. Yuen, B. C. Das, K. Shudo, H. Kagechika, R. L. Leibel, W. S. Blaner, Retinoic acid receptor signaling is required to maintain glucose-stimulated insulin secretion and β-cell mass. *FASEB J.* **29**, 671–683 (2015).
12. S. E. Trasino, X.-H. Tang, J. Jessurun, L. J. Gudas, A retinoic acid receptor β2 agonist reduces hepatic stellate cell activation in nonalcoholic fatty liver disease. *J. Mol. Med.* **94**, 1143–1151 (2016).
13. E. Cortes, D. Lachowski, A. Rice, A. Chronopoulos, B. Robinson, S. Thorpe, D. A. Lee, L. A. Possamai, H. Wang, D. J. Pinato, A. E. del Río Hernández, Retinoic acid receptor-β is downregulated in hepatocellular carcinoma and cirrhosis and its expression inhibits myosin-driven activation and durotaxis in hepatic stellate cells. *Hepatology* **69**, 785–802 (2018).
14. Q. Yang, T. E. Graham, N. Mody, F. Preitner, O. D. Peroni, J. M. Zabolotny, K. Kotani, L. Quadro, B. B. Kahn, Serum retinol binding protein 4 contributes to insulin resistance in obesity and type 2 diabetes. *Nature* **436**, 356–362 (2005).
15. T. E. Graham, Q. Yang, M. Blüher, A. Hammarstedt, T. P. Ciaraldi, R. R. Henry, C. J. Wason, A. Oberbach, P.-A. Jansson, U. Smith, B. B. Kahn, Retinol-binding protein 4 and insulin resistance in lean, obese, and diabetic subject. *N. Engl. J. Med.* **354**, 2552–2563 (2006).
16. X. Terra, T. Auguet, M. Broch, F. Sabech, M. Hernández, R. M. Pastor, I. M. Quesada, A. Luna, C. Aguilar, D. del Castillo, C. Richart, Retinol binding protein-4 circulating levels were higher in nonalcoholic fatty liver disease vs. histologically normal liver from morbidly obese women. *Obesity* **21**, 170–177 (2013).
17. K. M. Farjo, R. A. Farjo, S. Halsey, G. Moiseyev, J.-x. Ma, Retinol-binding protein 4 induces inflammation in human endothelial cells by an NADPH oxidase- and nuclear factor kappa B-dependent and retinol-independent mechanism. *Mol. Cell. Biol.* **32**, 5103–5115 (2012).
18. P. M. Moraes-Vieira, M. M. Yore, P. M. Dwyer, I. Syed, P. Aryal, B. B. Kahn, RBP4 activates antigen-presenting cells, leading to adipose tissue inflammation and systemic insulin resistance. *Cell Metab.* **19**, 512–526 (2014).
19. D. E. Ong, A novel retinol-binding protein from rat. Purification and partial characterization. *J. Biol. Chem.* **259**, 1476–1482 (1984).
20. A. M. Gajda, J. Storch, Enterocyte fatty acid-binding proteins (FABPs): Different functions of liver and intestinal FABPs in the intestine. *Prostaglandins Leukot. Essent. Fatty Acids* **93**, 9–16 (2015).

21. L. Cheng, S.-j. Qian, C. Rothschild, A. d'Avignon, J. B. Lefkowith, J. I. Gordon, E. Li, Alteration of the binding specificity of cellular retinol-binding protein II by site-directed mutagenesis. *J. Biol. Chem.* **266**, 24404–24412 (1991).
22. D. E. Ong, M. E. Newcomer, F. Chytil, Cellular retinoid-binding proteins, in *The Retinoids: Biology, Chemistry and Medicine*, M. B. Sporn, A. B. Roberts, D. S. Goodman, Eds. (Raven Press Ltd., ed. 2, 1994), pp. 283–318.
23. X. E, L. Zhang, J. Lu, P. Tso, W. S. Blaner, M. S. Levin, E. Li, Increased neonatal mortality in mice lacking cellular retinol-binding protein II. *J. Biol. Chem.* **277**, 36617–36623 (2002).
24. N. Wongsiriroj, R. Piantedosi, K. Palczewski, I. J. Goldberg, T. P. Johnston, E. Li, W. S. Blaner, The molecular basis of retinoid absorption: A genetic dissection. *J. Biol. Chem.* **283**, 13510–13519 (2008).
25. X.-H. Tang, L. J. Gudas, Retinoids, retinoic acid receptors, and cancer. *Annu. Rev. Pathol.* **6**, 345–364 (2011).
26. M. Kaczocha, S. T. Glaser, D. G. Deutsch, Identification of intracellular carriers of the endocannabinoid anadamide. *Proc. Natl. Acad. Sci. U.S.A.* **106**, 6375–6380 (2009).
27. E. P. Newberry, S. M. Kennedy, Y. Xie, J. Luo, R. M. Crooke, M. J. Graham, J. Fu, D. Piomelli, N. O. Davidson, Decreased body weight and hepatic steatosis with altered fatty acid ethanolamide metabolism in aged *L-Fapb*$^{-/-}$ mice. *J. Lipid Res.* **53**, 744–754 (2012).
28. W. S. Lagakos, X. Guan, S.-Y. Ho, I. Rodriguez Sawicki, B. Corsino, S. Kodukula, K. Murota, R. E. Stark, J. Storch, Liver fatty acid-binding protein binds monoacylglycerol in vitro and in mouse liver cytosol. *J. Biol. Chem.* **288**, 19805–19815 (2013).
29. M. Kaczocha, S. Vivieca, J. Sun, S. T. Glaser, D. G. Deutsch, Fatty acid-binding proteins transport *N*-acylethanolamines to nuclear receptors and are targets of endocannabinoid transport inhibitors. *J. Biol. Chem.* **287**, 3415–3424 (2012).
30. A. E. Thumser, J. B. Moore, N. J. Plant, Fatty acid binding proteins: Tissue-specific functions in health and disease. *Curr. Opin. Clin. Nutr. Metab. Care* **17**, 124–129 (2014).
31. M. Kaczocha, M. J. Rebecchi, B. P. Ralph, Y.-H. G. Teng, W. T. Berger, W. Galbavy, M. W. Elmes, S. T. Glaser, L. Wang, R. C. Rizzo, D. G. Deutsch, I. Ojima, Inhibition of fatty acid binding proteins elevates brain anandamide levels and produces analgesia. *PLOS ONE* **9**, e94200 (2014).
32. P. G. Reeves, F. H. Nielsen, C. C. Fahey Jr., AIN-93 purified diets for laboratory rodents: Final report of the American Institute of Nutrition ad hoc writing committee on the reformulation of the AIN-76A rodent diet. *J. Nutr.* **123**, 1939–1951 (1993).
33. M. A. Kane, F. V. Bright, J. L. Napoli, Binding affinities of CRBPI and CRBPII for 9-*cis*-retinoids. *Biochim. Biophys. Acta* **1810**, 514–518 (2011).
34. C.-L. E. Yen, D. W. Nelson, M.-I. Yen, Intestinal triacylglycerol synthesis in fat absorption and systemic energy metabolism. *J. Lipid Res.* **56**, 489–501 (2015).
35. S.-H. Chon, J. D. Douglass, Y. X. Zhou, N. Malik, J. L. Dixon, A. Brinker, L. Quadro, J. Storch, Over-expression of monoacylglycerol lipase (MGL) in small intestine alters endocannabinoid levels and whole body energy balance, resulting in obesity. *PLOS ONE* **7**, e43962 (2012).
36. J. D. Douglass, Y. X. Zhou, A. Wu, J. A. Zadrogra, A. M. Gajda, A. I. Lackey, W. Lang, K. M. Chevalier, S. W. Sutton, S.-P. Zhang, C. M. Flores, M. A. Connelly, J. Storch, Global deletion of MGL in mice delays lipid absorption and alters energy homeostasis and diet-induced obesity. *J. Lipid Res.* **56**, 1153–1171 (2015).
37. C. H. S. McIntosh, S. Widenmaier, S.-J. Kim, Glucose-dependent insulinotropic polypeptide (gastric inhibitory polypeptide; GIP). *Vitam. Horm.* **80**, 409–471 (2009).
38. K. B. Hansen, M. M. Rosenkilde, F. K. Knop, N. Wellner, T. A. Diep, J. F. Rehfeld, U. B. Anderson, J. J. Holst, H. S. Hansen, 2-Oleoyl glycerol is a GRP119 agonist and signals GLP-1 release in humans. *J. Clin. Endocrinol. Metab.* **96**, E1409–E1417 (2011).
39. J. H. Ekberg, M. Hauge, L. V. Kristensen, A. N. Madsen, M. S. Engelstoft, A.-S. Husted, R. Sichlau, K. L. Egerod, P. Timshel, T. J. Kowalski, F. M. Gribble, F. Reiman, H. S. Hansen, B. Holst, T. W. Schwartz, GRP119, a major enteroendocrine sensor of dietary triglyceride metabolites coacting in synergy with FFA1 (GPR40). *Endocrinology* **157**, 4561–4569 (2016).
40. D. Chanda, D. Neumann, J. F. C. Glatz, The endocannabinoid system: Overview of an emerging multi-faceted therapeutic target. *Prostaglandins Leukot. Essent. Fatty Acids* **140**, 51–56 (2019).
41. C. W. Chia, O. D. Carlson, D. D. Liu, I. González-Mariscal, S. Santa-Cruz Calvo, J. M. Egan, Incretin secretion in humans is under the influence of cannabinoid receptors. *Am. J. Physiol. Endocrinol. Metab.* **333**, E359–E366 (2017).
42. M. J. Theodorakis, O. Carlson, D. C. Muller, J. M. Egan, Elevated plasma glucose-dependent insulinotropic polypeptide associates with hyperinsulinemia in impaired glucose tolerance. *Diabetes Care* **27**, 1692–1698 (2004).
43. S. Calanna, M. Christensen, J. J. Holst, B. Lafèrrere, L. L. Gluud, T. Vilsbøll, F. K. Knop, Secretion of glucose-dependent insulinotropic polypeptide in patients with type 2 diabetes: Systematic review and meta-analysis of clinical studies. *Diabetes Care* **36**, 3346–3352 (2013).
44. E. W. L. Sun, A. M. Martin, R. L. Young, D. J. Keating, The regulation of peripheral metabolism by gut-derived hormones. *Front. Endocrinol.* **9**, 754 (2019).
45. K. Miyawaki, Y. Yamada, N. Ban, Y. Ihara, K. Tsukiyama, H. Zhou, S. Fujimoto, A. Oku, K. Tsuda, S. Toykuni, H. Hiai, W. Mizunoya, T. Fushiki, J. J. Holst, M. Makino, A. Tashita, Y. Kobara, Y. Tsubamoto, T. Jinnouchi, T. Jomori, Y. Seino, Inhibition of gastric inhibitory polypeptide signaling prevents obesity. *Nat. Med.* **8**, 738–742 (2002).
46. F. Isken, A. F. H. Pfeiffer, R. Nogueiras, M. A. Osterhoff, M. Ristow, B. Thorens, M. H. Tschöp, M. O. Weickert, Deficiency of glucose-dependent insulinotropic polypeptide receptor prevents ovariectomy-induced obesity in mice. *Am. J. Physiol. Endocrinol. Metab.* **295**, E350–E355 (2008).
47. E. A. Killion, J. Wang, J. Yie, S. D.-H. Shi, D. Bates, X. Min, R. Komorowski, T. Hager, L. Deng, L. Atangan, S.-C. Lu, R. J. M. Kurzeja, G. Sivits, J. Lin, Q. Chen, Z. Wang, S. A. Thibault, C. M. Abbott, T. Meng, B. Clavette, C. M. Murawsky, I. N. Foltz, J. B. Rottman, C. Hale, M. M. Véniant, D. J. Lloyd, Anti-obesity effects of GIPR antagonists alone and in combination with GLP-1R agonists in preclinical models. *Sci. Transl. Med.* **10**, pii: eaat3392 (2018).
48. S.-J. Kim, C. Nian, C. H. S. McIntosh, Activation of lipoprotein lipase by glucose-dependent insulinotropic polypeptide in adipocytes. *J. Biol. Chem.* **282**, 8557–8567 (2007).
49. S.-J. Kim, C. Nian, C. H. S. McIntosh, GIP increases human adipocyte LPL expression through CREB and TORC2-mediated *trans*-activation of the *LPL* gene. *J. Lipid Res.* **51**, 3145–3157 (2010).
50. M. Rubinstein, M. J. Low, Molecular and functional genetics of the proopiomelanocortin gene, food intake regulation and obesity. *FEBS Lett.* **591**, 2593–2606 (2017).
51. H. S. Hansen, V. Vana, Non-endocannabinoid *N*-acylethanolamines and 2-monoacylglycerols in the intestine. *Br. J. Pharmacol.* **176**, 1443–1454 (2019).
52. E. Harno, T. Gali Ramamoorthy, A. P. Coll, A. White, POMC: The physiological power of hormone processing. *Physiol. Rev.* **98**, 2381–2430 (2018).
53. J. Storch, B. Corsinco, The emerging functions and mechanisms of mammalian fatty acid–binding proteins. *Annu. Rev. Nutr.* **28**, 73–95 (2008).
54. G. S. Hotamisligil, D. A. Bernlohr, Metabolic functions of FABPs—Mechanisms and therapeutic implications. *Nat. Rev. Endocrinol.* **11**, 592–605 (2015).
55. A. M. Gajda, Y. X. Zhou, L. B. Agellon, S. K. Fried, S. Kodukula, W. Fortson, K. Patel, J. Storch, Direct comparison of null mice for liver or intestinal fatty acid-binding proteins reveals highly divergent phenotypic responses to high fat feeding. *J. Biol. Chem.* **288**, 30330–30344 (2013).
56. M. Golczak, P. D. Kiser, A. E. Sears, D. T. Lodowski, W. S. Blaner, K. Palczewski, Structural basis for the acyltransferase activity of lecithin:retinol acyltransferase-like proteins. *J. Biol. Chem.* **287**, 23790–23807 (2012).
57. R. E. Duncan, E. Sarkadi-Nagy, K. Jaworski, M. Ahmadian, H. S. Sul, Identification and functional characterization of adipose-specific phospholipase A_2 (AdPLA). *J. Biol. Chem.* **283**, 25428–25436 (2008).
58. N. Wongsiriroj, H. Jiang, R. Piantedosi, K. J. Z. Yang, J. Kluwe, R. F. Schwabe, H. Ginsberg, I. J. Goldberg, W. S. Blaner, Genetic dissection of retinoid esterification and accumulation in the liver and adipose tissue. *J. Lipid Res.* **55**, 104–114 (2014).
59. R. D. Clugston, H. Jiang, M. X. Lee, R. Piantedosi, J. J. Yuen, R. Ramakrishnan, M. J. Lewis, M. E. Gottesman, L.-S. Huang, I. J. Goldberg, P. D. Berk, W. S. Blaner, Altered hepatic lipid metabolism in C57BL/6 mice fed alcohol: A targeted lipidomic and gene expression study. *J. Lipid Res.* **52**, 2021–2031 (2011).
60. National Research Council. *Guide for the Care and Use of Laboratory Animals* (National Academies Press, ed. 8, 2011).
61. A. B. Barua, H. C. Furr, Properties of retinoids. Structure, handling and preparation. *Mol. Biotechnol.* **10**, 167–182 (1998).
62. M. A. Kane, A. E. Folias, C. Wang, J. L. Napoli, Quantitative profiling of endogenous retinoic acid in vivo and in vitro by tandem mass spectrometry. *Anal. Chem.* **80**, 1702–1708 (2008).
63. J. A. Silvaroli, M. A. K. Widjaja-Adhi, T. Trishman, S. Chelstowska, S. Horwitz, S. Banerjee, P. D. Kiser, W. S. Blaner, M. Golczak, Abnormal cannabidiol modulates vitamin A metabolism by acting as a competitive inhibitor of CRBP1. *ACS Chem. Biol.* **14**, 434–448 (2019).
64. W. Kabsch, Integration, scaling, space-group assignment and post-refinement. *Acta Crystallogr. D Biol. Crystallogr.* **66**, 133–144 (2010).
65. F. Long, A. A. Vagin, P. Young, G. N. Murshudov, BALBES: A molecular-replacement pipeline. *Acta Crystallogr. D Biol. Crystallogr.* **64**, 125–132 (2008).
66. P. Emsley, K. Cowtan, Coot: model-building tools for molecular graphics. *Acta Crystallogr. D Biol. Crystallogr.* **60**, 2126–2132 (2004).
67. P. D. Adams, P. V. Afonine, G. Bunkóczi, V. B. Chen, I. W. Davis, N. Echols, J. J. Headd, L.-W. Hung, G. J. Kapral, R. W. Grosse-Kunstleve, A. J. McCoy, N. W. Moriarty, R. Oeffner, R. J. Read, D. C. Richardson, J. S. Richardson, T. C. Terwilliger, P. H. Zwart, PHENIX: A comprehensive Python-based system for macromolecular structure solution. *Acta Crystallogr. D Biol. Crystallogr.* **66**, 213–221 (2010).
68. V. B. Chen, W. B. Arendall III, J. J. Headd, D. A. Keedy, R. M. Immormino, G. J. Kapral, L. W. Murray, J. S. Richardson, D. C. Richardson, MolProbity: All-atom structure validation for macromolecular crystallography. *Acta Crystallogr. D Biol. Crystallogr.* **66**, 12–21 (2010).
69. E. F. Pettersen, T. D. Goddard, C. C. Huang, G. S. Couch, D. M. Greenblatt, E. C. Meng, T. E. Ferrin, UCSF Chimera—A visualization system for exploratory research and analysis. *J. Comput. Chem.* **25**, 1605–1612 (2004).

70. N. R. Blumenfeld, H. J. Kang, A. Fenzyl, Z. Song, J. J. Chung, R. Singh, R. Johnson, A. Karakecili, J. B. Feranil, N. S. Rossen, V. Zhang, S. Jaggi, B. McCarty, S. Bessler, G. J. Schwartz, R. Grant, J. Korner, F. W. Kiefer, B. M. Gillette, S. K. Sia, A direct tissue-grafting approach to increasing endogenous brown fat. *Sci. Rep.* **8**, 7957 (2018).

Acknowledgments: We thank F. Mancia for helping with the original in silico studies exploring the possibility of 2-MAG binding to RBP2 and D. T. Lodowski for assistance in collecting the x-ray diffraction data. We also thank E. Li who read this manuscript before its submission and provided comments and suggestions regarding the work and manuscript. **Funding:** This work was supported by grants R01DK068437 (to W.S.B.), R01DK101251 (to W.S.B.), R01EY023948 (to M.G.), R01DK122071 (to W.S.B. and M.G.), P30DK026687 (to R.L.), R01DK052431 (to R.L.L.), R01DK038389 (to J.S.), T32DK007647 (to X.L.), and T32DK007328 (to X.L.) from the U.S. Public Health Services, NIH and from the University of Strasbourg Institute for Advanced Study (to W.K.). This work is based on research conducted at the Northeastern Collaborative Access Team beamlines, which are funded by the National Institute of General Medical Sciences from the NIH (P30 GM124165). The Pilatus 6M detector on 24-ID-C beam line is funded by NIH-ORIP-HEI grant (S10 RR029205). This research used resources of the Advanced Photon Source, a U.S. Department of Energy (DOE) Office of Science User Facility operated for the DOE Office of Science by Argonne National Laboratory under contract no. DE-AC02-06CH11357.
Author contributions: S.-A.L., K.J.Z.Y., P.-J.B., J.A.S., J.J.Y., I.S., H.J., X.L., and J.B.F. carried out experiments, contributed to the design of experiments, discussed research plans and data, and helped write and edit the manuscript. A.I.L. contributed to the design of the experiments and edited the manuscript. J.L., W.K., J.S., and R.L.L. contributed to the design of experiments, discussed research plans and data, and edited the manuscript. M.G. carried out experiments, contributed to the design of experiments, discussed research plans and data, edited the manuscript, and provided research support for the studies. W.S.B. contributed to the design of experiments, discussed research plans and data, wrote the first and edited subsequent drafts of the manuscript, and provided research support for the studies. **Competing interests:** The authors declare that they have no competing interests. **Data and materials availability:** All data needed to evaluate the conclusions in the paper are present in the paper and/or the Supplementary Materials. The structural data reported in the manuscript have been deposited in and are available through the wwPDB (accession numbers 6BTH and 6BTI). Additional data related to this paper may be requested from the authors.

Submitted 26 July 2019
Accepted 16 December 2019
Published 11 March 2020
10.1126/sciadv.aay8937

Citation: S.-A. Lee, K. J. Z. Yang, P.-J. Brun, J. A. Silvaroli, J. J. Yuen, I. Shmarakov, H. Jiang, J. B. Feranil, X. Li, A. I. Lackey, W. Krężel, R. L. Leibel, J. Libien, J. Storch, M. Golczak, W. S. Blaner, Retinol-binding protein 2 (RBP2) binds monoacylglycerols and modulates gut endocrine signaling and body weight. *Sci. Adv.* **6**, eaay8937 (2020).

ScienceAdvances

Retinol-binding protein 2 (RBP2) binds monoacylglycerols and modulates gut endocrine signaling and body weight

Seung-Ah LeeKryscilla Jian Zhang YangPierre-Jacques BrunJosie A. SilvaroliJason J. YuenIgor ShmarakovHongfeng JiangJun B. FeranilXueting LiAtreju I. LackeyWojciech Kr##elRudolph L. LeibelJenny LibienJudith StorchMarcin GolczakWilliam S. Blaner

Sci. Adv., 6 (11), eaay8937. • DOI: 10.1126/sciadv.aay8937

Science Advances (ISSN 2375-2548) is published by the American Association for the Advancement of Science. 1200 New York Avenue NW, Washington, DC 20005. The title *Science Advances* is a registered trademark of AAAS.